

ORIGINAL ARTICLE

Activation of Annexin A2 signaling at the blood–brain barrier in a mouse model of multiple sclerosis

Kenta Tezuka | Masayoshi Suzuki | Risa Sato | Shohei Kawarada | Tetsuya Terasaki  | Yasuo Uchida 

Graduate School of Pharmaceutical Sciences, Tohoku University, Sendai, Japan

Correspondence

Yasuo Uchida, Division of Membrane Transport and Drug Targeting, Graduate School of Pharmaceutical Sciences, Tohoku University, 6-3 Aoba, Aramaki, Aoba-ku, Sendai 980-8578, Japan.
Email: yasuo.uchida.c8@tohoku.ac.jp

Funding information

Japan Society for the Promotion of Science, Grant/Award Number: KAKENHI, 18KK0446 and 20H03399; Ministry of Education, Culture, Sports, Science and Technology, Grant/Award Number: 20H04690 and 20H05495

Abstract

Blood–brain barrier (BBB) dysfunction is a fundamental cause of multiple sclerosis and identifying the molecules that are responsible is an urgent matter. Protein expression was comprehensively quantified at the BBB of experimental autoimmune encephalomyelitis (EAE) mice, a model of multiple sclerosis, using the SWATH method. Concerning tight junction molecules, the level of expression of Claudin-5, which, in a previous immunohistochemical analysis, was confirmed to be down-regulated by EAE, remained unchanged, but the expression of Claudin-11 and Occludin was decreased by 0.69- and 0.62-fold, respectively, in brain capillaries isolated from EAE mice. A number of other cell–cell junctional molecules including ESAM, CADM1, CADM2, CADM3, CADM4, and HEPACAM were also down-regulated. The levels of expression of intercellular adhesion molecule 1 (ICAM1) and vascular cell adhesion molecule 1 (VCAM1), which directly mediate the infiltration of lymphocytes across the BBB, were increased in EAE mice by 3.3- and 2.6-fold, respectively. The expression of CXADR, which possibly facilitates the adhesion of migrating cells, was also increased by 3.5-fold. Interestingly, various members of the Annexin A (ANXA) family were also up-regulated in brain capillaries that were isolated from EAE mice. In a pathway associated with cell infiltration and tight junction disruption, a series of molecules that are involved in ANXA2 signaling (ANXA2, PTP1B, Ahnak, S100A11, CD44, Kindlin2, Integrin α 5, Fibronectin, Fibrinogen) were up-regulated. ANXA2 is selectively and abundantly expressed in endothelial cells in the brain. The daily administration of an ANXA2 inhibitor (LCKLSL peptide) significantly suppressed the development of EAE in mice. In summary, the activation of ANXA2 signaling at the BBB appear to play an important role in the pathogenesis of EAE.

KEYWORDS

Annexin A2, blood–brain barrier, cell infiltration, multiple sclerosis, SWATH, tight junction

Abbreviations: ANXA2, Annexin A2; BBB, blood–brain barrier; B-cap, brain capillary; CNS, central nervous system; EAE, experimental autoimmune encephalomyelitis; ICAM1, intercellular adhesion molecule 1; LC-MS/MS, liquid chromatography–tandem mass spectrometry; qTAP, quantitative Targeted Absolute Proteomics; SWATH-MS, sequential window acquisition of all theoretical fragment ion spectra mass spectrometry; VCAM1, vascular cell adhesion molecule 1.



1 | INTRODUCTION

The migration of lymphocytes across the blood–brain barrier (BBB), which consists of brain capillary endothelial cells that are linked by complex tight junctions, is an important step in the progression of brain dysfunction during multiple sclerosis. Suppressing lymphocytic infiltration is an important strategy in the treatment of multiple sclerosis. Accumulating evidence suggests that lymphocyte migration involves membrane proteins in brain capillary endothelial cells, which mediate the opening of tight junctions, the sequential processes involve the activation of lymphocytes, lymphocyte-endothelial cell adhesion, and the transmigration of lymphocytes across endothelial cells (Engelhardt & Ransohoff, 2012; Rossi et al., 2011). To identify promising drugs for the treatment of multiple sclerosis, it is important to explore the molecular mechanisms responsible for the infiltration of lymphocytes into the brain and quantitatively clarifying the importance of individual molecules.

Claudin-5 is an important tight junction molecule that functions at the BBB. Based on an immunohistochemical analysis, it was reported that the expression of Claudin-5 at the BBB is decreased in experimental autoimmune encephalomyelitis (EAE) mice, a model of multiple sclerosis, and it has been identified as a molecule responsible for the disruption of tight junctions in multiple sclerosis (Argaw et al., 2009). However, quantitative Targeted Absolute Proteomics (qTAP), which is quantitatively more accurate than antibody-based analyses, has shown that the level of expression of Claudin-5 in the brain capillaries of EAE mice is nearly the same as that in normal mice (Sato et al., 2019). Therefore, the issue of whether Claudin-5 is actually the cause of the disruption of tight junctions remains an open question. We recently reported that Claudin-11 functions as a new tight junction molecule at the BBB and that it is expressed more abundantly than Claudin-5 at the human BBB (Uchida et al., 2019). Our findings also indicate that Claudin-11 is down-regulated in multiple sclerosis and contributes to barrier disruption. However, this conclusion was based on an analysis using antibodies, and the question remains as to how much the protein expression level is reduced. An important issue remaining is to quantitatively understand the extent to which Claudin-5, -11, and other tight junction/adhesion molecules contribute to barrier disruption in multiple sclerosis.

In addition to the opening of tight junctions, membrane proteins that promote lymphocyte adhesion and infiltration also play an important role, but it is not clear which specific molecules contribute and to what extent, because there are almost no studies that have comprehensively and quantitatively evaluated these membrane proteins. It was reported, based on an immunohistochemical analysis, that the expression of CD54/intercellular adhesion molecule 1 (ICAM1) and CD106/vascular cell adhesion molecule 1 (VCAM1), proteins that are thought to be involved in lymphocyte infiltration, is increased at the BBB in multiple sclerosis (Bö et al., 1996; Huang et al., 2017; Steffen et al., 1994; Washington et al., 1994). However, qTAP analyses have shown that the expression levels of these proteins in brain capillaries of EAE mice are nearly the same as the values for normal mice (Sato et al., 2019). Although the quantitative

accuracy of the qTAP method is superior to that of an antibody-based analysis, only one tryptic peptide (not the entire sequence of the protein) was used to quantify the target protein in this report, so it cannot be said with certainty that the expressions of CD54/ICAM1 and CD106/VCAM1 are not actually up-regulated. In addition to CD54/ICAM1 and CD106/VCAM1, various other membrane proteins and related molecules at the BBB are involved in the invasion of lymphocytes into the central nervous system (CNS) tissues. Regarding identifying promising drug targets, comprehensively and quantitatively elucidating how much all of these related molecules including CD54/ICAM1 and CD106/VCAM1 contribute to the invasion is an important issue.

The SWATH method is one of the more recently developed comprehensive quantitative proteomics methods, and its excellent quantitative accuracy as compared with previous comprehensive proteomics is a significant advantage (Gillet et al., 2012). Multiple specific peptides derived from a single protein can be quantified, and the change in the level of expression of the target protein can be quantified based on the average of these peptides. Membrane proteins contain hydrophobic regions, such as transmembrane sites, which cause their incomplete solubilization and resistance to trypsin digestion. However, we were able to improve the accuracy of the SWATH method by completely solubilizing such proteins with guanidine hydrochloride, thus improving the efficiency of the tryptic digestion of membrane proteins (Uchida et al., 2020a), and by applying *in silico* peptide selection criteria (Kamie et al., 2008), such as excluding transmembrane sites and sequences with poor tryptic digestion efficiency from the numerous peptides that are measured (Uchida et al., 2021; Uchida et al., 2020b).

The purpose of the present study was to comprehensively quantify the protein expression at the BBB of EAE mice, a model of multiple sclerosis, using the SWATH method, and to then identify the molecules responsible for EAE pathogenesis.

2 | MATERIALS AND METHODS

2.1 | EAE mice

EAE Induction Hooke Kits (Catalogue Number EK-2110, Hooke Laboratories, Lawrence, MA, USA) were used for EAE induction according to the manufacturer's instructions, as previously described (Uchida et al., 2019). The animal experiments were conducted based on ARRIVE guidelines, and the protocol was approved by the Institutional Animal Care and Use Committee at Tohoku University (Approval Code, 2016PhA-040). The present study was not pre-registered.

For SWATH experiments, EAE was induced in 10-week-old female C57BL/6J mice. The mice were immunized subcutaneously in the neck and lower back (0.1 ml/site, total of 0.2 ml) on Day 0 with 100 µg of MOG_{35–55} peptide emulsified in complete Freund's adjuvant. Each mouse was injected intraperitoneally with 200 ng of pertussis toxin at 0.1 ml/dose at 2 and 24 h after immunization (total of



400 ng). The progression of EAE was evaluated by scoring the clinical symptoms. Mice with a clinical score of 3.5 to 4.0 on Day 16 after immunization with the MOG_{35–55} peptide were used in the experiments.

For experiments with the LCKLSL peptide, 12-week-old female C57BL/6J mice were used. Mice received daily intraperitoneal injections of the LCKLSL peptide (Catalogue Number HY-P2333A, MedChemExpress, Monmouth Junction, NJ, USA) with 5 mg/kg/day (six mice), or vehicle (PBS) for the control group (three mice) without anesthesia, from 7 days before immunization with the MOG_{35–55} peptide. The induction and scoring of EAE were conducted with same procedure as above. The daily injections of LCKLSL peptide or PBS (control) were continued until Day 23 after immunization with the MOG_{35–55} peptide. Mice were finally killed by cervical dislocation.

Mice were maintained on a 12-h light/dark cycle in a temperature-controlled environment with free access to food and water in conventional cages. After immunization, the mice were maintained with one mouse per cage and the animal bedding in the cage was not exchanged until the series of experiments was completed to minimize the stress. After the onset of EAE, dietgel and hydrogel were also given to the mice in addition to normal food and water so that the mice would be able to have easy access to the food and water.

2.2 | Isolation of brain capillaries (B-cap)

Mouse brain capillaries were isolated as previously described with minor modifications (Uchida et al., 2020c). Briefly, mice received a cardiac perfusion with PBS under isoflurane anesthesia (which is appropriate for safe anesthesia in a short time), and the cerebrum was then excised after decapitation. The cerebrums were minced 80 times/g wet of tissue with scissors (Catalogue Number NAPOX B-5H, Natsume Seisakusho, Tokyo, Japan) and 160 times/g of wet tissue with smaller scissors (Catalogue Number NAPOX B-12H, Natsume Seisakusho, Tokyo, Japan). The minced cerebrum was homogenized in a Potter-Elvehjem homogenizer using 120 up-and-down unrotated strokes by hand in 5 volumes of solution B (101-mM NaCl, 4.6-mM KCl, 2.5-mM CaCl₂, 1.2-mM KH₂PO₄, 1.2-mM MgSO₄, 15-mM HEPES, pH 7.4) per brain weight. The homogenate was centrifuged (1000 g, 4°C, 10 min) and the supernatant was removed. The pellet was suspended in solution B containing 22.5% dextran (Catalogue Number 18693.02, SERVA Electrophoresis GmbH, Heidelberg, Germany), and the suspension was centrifuged (5800 g, 4°C, 15 min). The resulting pellet was suspended in 10 ml of solution A (solution B containing 25-mM NaHCO₃, 10-mM glucose, 1-mM pyruvate, 5 g/L of bovine serum albumin). The suspension was passed through a 210-μm nylon mesh (Catalogue Number NRK-210, Nippon Rikagaku Kikai CO. LTD., Tokyo, Japan), and the mesh was washed with 20 ml of solution A. The filtrate was passed over a column containing 350–500 μm of glass beads (Catalogue Number BZ-04, AS ONE Corporation, Osaka, Japan) and washed with 30 ml of solution A per g brain. The microvessels adhering to the beads were detached in solution A, and, as soon as the tissue was released, the supernatant including the microvessels was collected. The pellet

obtained by centrifugation (1000 g, 4°C, 5 min) was resuspended in solution B and centrifuged again (1000 g, 4°C, 5 min). The resulting pellet was resuspended in solution B. A part of the suspension was stained with trypan blue and observed with a Leica CTR 6000 (Leica Microsystems) to evaluate the purity of the brain capillaries. The capillary suspension was then centrifuged (1000 g, 4°C, 5 min), and the resulting pellet was suspended in hypotonic buffer. The total amount of protein in the suspension containing the cerebrum capillaries was measured by the Lowry method using a DC protein assay kit (Catalogue Numbers 5000113 and 5000114, Bio-Rad). A Model 680 microplate reader (Bio-Rad) was used to measure the absorbance. The brain capillaries were stored at –80°C until used.

We confirmed that the vascular structure was maintained by microscopic examination of the isolated vessel samples (Figure S1). An absolute protein quantification analysis of vessels that were isolated by the same previously reported method showed that the proteins were localized at the luminal membrane and abluminal membrane and that the level of protein expression at the tight junctions of brain capillary endothelial cells was of the same order (Uchida et al., 2013). This suggests that the structure and protein expression of the endothelial cells is maintained during the capillary isolation procedure.

2.3 | Sample preparation for SWATH-based quantitative proteomics

Protein digestion was performed as described previously (Uchida et al., 2013). Briefly, 50 μg of isolated brain capillaries was solubilized in denaturing buffer (7-M guanidium hydrochloride, 0.5-M Tris-HCl [pH 8.5], 10-mM EDTA). The solubilized proteins were reduced by treatment with dithiothreitol for 1 h at 25°C and then S-carboxymethylated with iodoacetamide for 1 h at 25°C in the dark. The alkylated proteins were precipitated with a methanol-chloroform-water mixture. The precipitates were solubilized in 6-M urea in 0.1-M Tris-HCl (pH 8.5) and diluted fivefold with 0.1 M Tris-HCl (pH 8.5) containing 0.05% ProteaseMax surfactant (Catalogue Number V2072, Promega, Madison, WI, USA). The dilutions were reacted with lysyl endopeptidase (Lys-C; Catalogue Number 129-02541, Wako Pure Chemical Industries, Osaka, Japan) at an enzyme/substrate ratio of 1 : 100 for 3 h at 30°C. The Lys-C digested proteins were subsequently treated with TPCK-treated trypsin (Catalogue Number V5113, Promega, Madison, WI, USA) at an enzyme/substrate ratio of 1 : 100 for 16 h at 37°C. The tryptic digests were cleaned up with a self-packed SDB-XD 200 μl tip (Catalogue Number 2242, 3 M, Minnesota) as previously described (Uchida et al., 2019).

2.4 | LC-MS/MS measurement for SWATH-based quantitative proteomics

The cleaned peptide samples were injected into a NanoLC 425 system (Eksigent Technologies, Dublin, CA, USA) coupled with an electrospray-ionization Triple TOF 5600 mass spectrometer



(SCIEX, Framingham, MA, USA), which was set up for a single direct injection and analyzed by SWATH-MS acquisition, as previously described (Uchida et al., 2020b). The peptides were directly loaded onto a self-packed 20-cm-long C18 analytical column, prepared by packing ProntoSIL 200-3-C18 AQ beads (Catalogue Number 0001H184PS030, 3 μ m, 120 Å, BISCHOFF Chromatography, Germany) in a PicoFrit tip (ID 75 μ m, Catalogue Number PF360-75-10-N5, New Objective). After sample loading, the peptides were separated and eluted with a linear gradient; 98% A : 2% B to 65% A : 35% B (0–120 min), increase to 0% A : 100% B (120–121 min), maintained at 0% A : 100% B (121–125 min), reduced to 98% A : 2% B (125–126 min), and then maintained at 98% A : 2% B (126–155 min). The composition of mobile phase A was 0.1% formic acid in water, and that for mobile phase B was 0.1% formic acid in acetonitrile. The flow rate was 300 nL/min. The eluted peptides were positively ionized and measured in the SWATH mode. The measurement parameters were as follows: SWATH window, 64 variable windows from 400 to 1200 m/z; product ion scan range, 50–2000 m/z; declustering potential, 100; rolling collision energy value, $0.0625 \times [\text{m/z of each SWATH window}] - 3.5$; collision energy spread, 15; accumulation time, 0.05 s for each SWATH window.

2.5 | Data analysis for SWATH-based quantitative proteomics

Spectral alignment and data extraction from the SWATH chromatogram (uploaded to the Peptide Atlas website with Identifier PASS01697) were performed with the SWATH Processing Micro App in Peakview (SCIEX) using in-house spectral libraries (uploaded to the Peptide Atlas website with Identifier PASS01697) as previously described (Uchida et al., 2020b). The parameters for peak data extraction by Peakview were described as follows: number of peptide per protein, 999; number of transitions per peptide, 6; peptide confidence threshold, 99%; false discovery rate (FDR) threshold, 1.0%; XIC extraction window, ± 4.0 min; XIC width (ppm), 50. According to the procedure previously described (Uchida et al., 2021), unreliable peaks and peptides were removed based on the criteria of data selection and amino acid sequence-based peptide selection, and the peak areas at the peptide level were calculated as an average of those in the transition level after normalizing the differences in signal intensity between the different transitions. The details were described in our previous study (Uchida et al., 2021). The peak areas of individual proteins were calculated as an average of those at the peptide level and were compared between EAE and control mouse groups.

2.6 | Statistical analysis

All statistical analyses were performed under the null hypothesis, assuming that the means for the compared groups were equal. Comparison between two groups was performed by an unpaired

two-tailed Student's *t*-test and followed by Benjamini–Hochberg (BH) correction. Exceptionally, the comparison between EAE mice that had been treated with the LCKLSL peptide and PBS involved the use of the two-tailed Mann–Whitney's *U* test, a non-parametric method. If the *p*-value was less than 0.05, the difference was considered to be statistically significant and the null hypothesis was rejected. A total of 19 mice were used (Figure S2). No formal power calculation was performed to estimate the required sample size. The number of subjects used for the present study was determined based on a previous study of a similar nature (Uchida et al., 2019). The normality of the data was not assessed. No randomization or blinding was performed in this study. No test for outliers was conducted. The flow chart of experimental procedure including the number of mice, sample processing, and measurement was shown in Figure S2.

3 | RESULTS

3.1 | Comprehensive protein quantification of brain capillaries isolated from EAE and normal mice by SWATH analysis

EAE was induced in C57BL/6J mice by administering the MOG_{35–55} peptide, and a 10-point clinical score was used to assess the severity of the EAE model. EAE began to develop at 13 days after immunization, and cerebral blood vessels were isolated from EAE mice with a score of 3.5 to 4.0 at Day 16 and used in the comprehensive quantitative proteomic analysis by SWATH (Figure 1a). Spectral alignment and data extraction from the SWATH chromatogram were performed with the SWATH Processing Micro App in Peakview software (SCIEX), as previously described (Uchida et al., 2020b). The parameters for peak data extraction by the Peakview software were as follows: number of peptides per protein, 999; number of transitions per peptide, 6; peptide confidence threshold, 99%; FDR threshold, 1.0%; XIC extraction window, ± 4.0 min; XIC width (ppm), 50. According to a previously reported procedure (Uchida et al., 2021), unreliable peaks and peptides were removed based on the criteria for data selection and amino acid sequence-based peptide selection. Median normalization was conducted to minimize the systematic error among six SWATH analyses (three EAE and three control runs). The peak areas at the peptide level were calculated as an average of those in the transition level after normalizing the differences in signal intensity between the different transitions. The details of this process were reported in our previous study (Uchida et al., 2021). The peak areas of individual proteins were calculated as an average of those at the peptide level and were compared between the EAE and control mouse groups (three EAE and three control runs).

A total of 2279 proteins were quantified (Table S1). Of these proteins, there were statistically significant differences between the EAE and normal groups for 528 of the proteins (BH-adjusted *p*-value < 0.05, Figure 1b; unpaired two-tailed Student's *t*-test, and followed by BH correction). The degree of freedom, *t*-value, *p*-value, and BH-adjusted *p*-value are listed in Table S1. Among them, 298

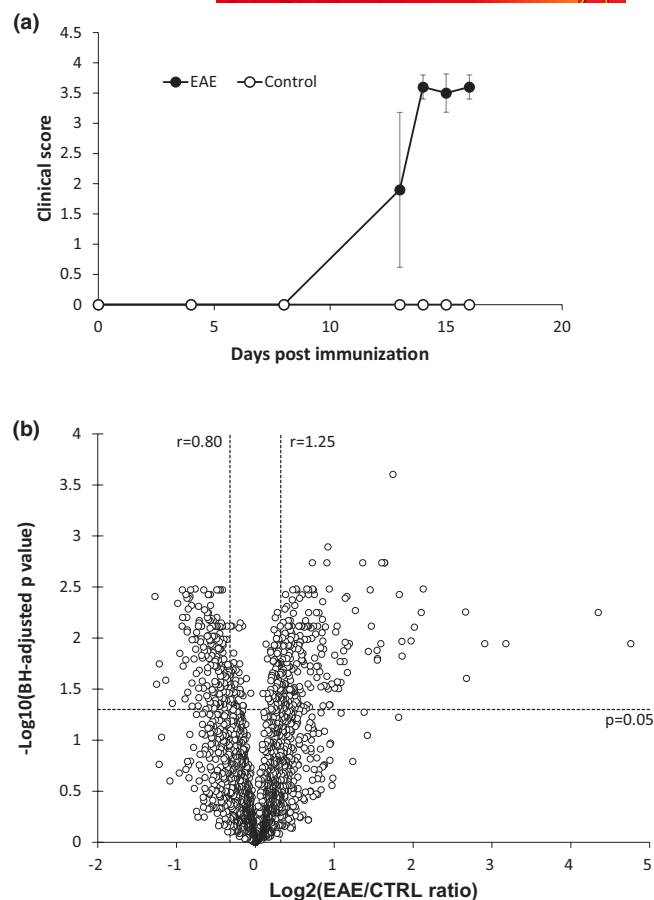


FIGURE 1 SWATH-based quantitative proteomics of brain capillaries isolated from EAE mice. (a) Time courses for the clinical scores of EAE mice after immunization with the MOG peptide and control (normal) mice. The progression of EAE was evaluated on Days 0, 4, 8, 13, 14, 15, and 16 by scoring clinical symptoms. Score 0, No clinical signs; Score 0.5, Tip of tail is limp; Score 1.0, Limp tail; Score 1.5, Limp tail and hind leg inhibition; Score 2.0, Limp tail and weakness of hind legs; Score 2.5, Limp tail and dragging of hind legs; Score 3.0, Limp tail and complete paralysis of hind legs; Score 3.5, Limp tail, complete paralysis of hind legs, animal is unable to right itself when placed on its side, and hind legs are together on one side of the body; Score 4.0, Limp tail, complete hind leg and partial front leg paralysis; Score 4.5, Complete hind and partial front leg paralysis, no movement around the cage, not alert; Score 5.0, Spontaneously rolling in the cage or dead. The data are presented as the mean \pm SD (EAE $n = 5$ mice; control $n = 5$ mice). Closed circle, EAE group. Open circle, control group. (b) Volcano plot representation of the SWATH analysis of brain capillaries isolated from EAE mice with a clinical score of 3.5 to 4.0 and control mice on Day 16 ($n = 3$ independent sample processing/SWATH runs). Broken lines represent 0.05 of BH-adjusted p -value (unpaired two-tailed Student's t -test followed by BH correction) (y -axis), 1.25- and 0.8-fold changes (EAE/control ratio, r) in protein expression levels (x -axis)

proteins were elevated in EAE mice, and, in contrast, 230 proteins were decreased. Among the proteins that showed significant differences, 220 proteins were up-regulated by more than 1.25-fold in the EAE group compared with the normal group, while 188 proteins were down-regulated by less than 0.8-fold in the EAE group (Figure 1b). The detail of sample metadata is described in Table S2.

3.2 | EAE-induced changes in protein expression levels of molecules related to cell infiltration at the BBB

The expression levels of ICAM1 and VCAM1 in brain capillaries were elevated in the EAE group compared with the normal group by 3.35-fold and 2.57-fold, respectively (Figure 2a). These quantifications were performed for peptides at four and eight locations within the ICAM1 and VCAM1 protein sequences, respectively. These were peptides that met the *in silico* peptide selection criteria for sensitivity and accuracy (Figure 2b). The SWATH method, which was used in this study, can quantify the target protein using peptides obtained from multiple locations.

It is also important to investigate changes in the expression of other proteins that are involved in cell invasion, including the Integrin family. CD32, CD44, CD45, H2-L, H2-K1, Integrin $\alpha 3$, $\alpha 5$, and $\beta 4$ were significantly up-regulated in the EAE group by 4.37-, 2.92-, 7.51-, 3.62-, 3.55-, 1.22-, 1.62-, and 1.57-fold, respectively. The expression of Cxadr was 3.52-fold higher in the EAE group (Figure 2c,d).

3.3 | EAE-induced changes in the level of expression of tight junction and adhesion molecules at the BBB

To identify the molecules that are involved in the disruption of the BBB in EAE, we investigated the expression levels of molecules that are involved in tight and adherens junctions. No significant decrease in the level of expression of Claudin-5, the most important tight junction molecule based on findings reported in previous studies (Figure 3a), was found. In contrast, the level of expression of Claudin-11, a Claudin molecule that was recently reported to contribute to tight junction formation at the BBB, was significantly decreased (0.69-fold) in the EAE group (Figure 3a).

Concerning other tight junction molecules, the expression levels of Occludin (0.62-fold), Esam (0.78-fold), and Jam2 (0.79-fold) were significantly decreased in the EAE group (Figure 3b). Concerning molecules associated with the adherens junction, the expression levels of Cadm1, 2, 3, 4, and Hepacam (0.67-, 0.59-, 0.62-, 0.78-, and 0.75-fold, respectively) were significantly decreased in the EAE group (Figure 3c).

3.4 | Up-regulation of the expression of Annexin A family members and EAE-induced changes in the expression levels of Annexin A2-related molecules at the BBB

To explore the molecular mechanisms responsible for affecting BBB disruption and CNS cell infiltration in multiple sclerosis, we focused on protein families whose expression levels were highly variable. We found that the levels of expression of almost all members of

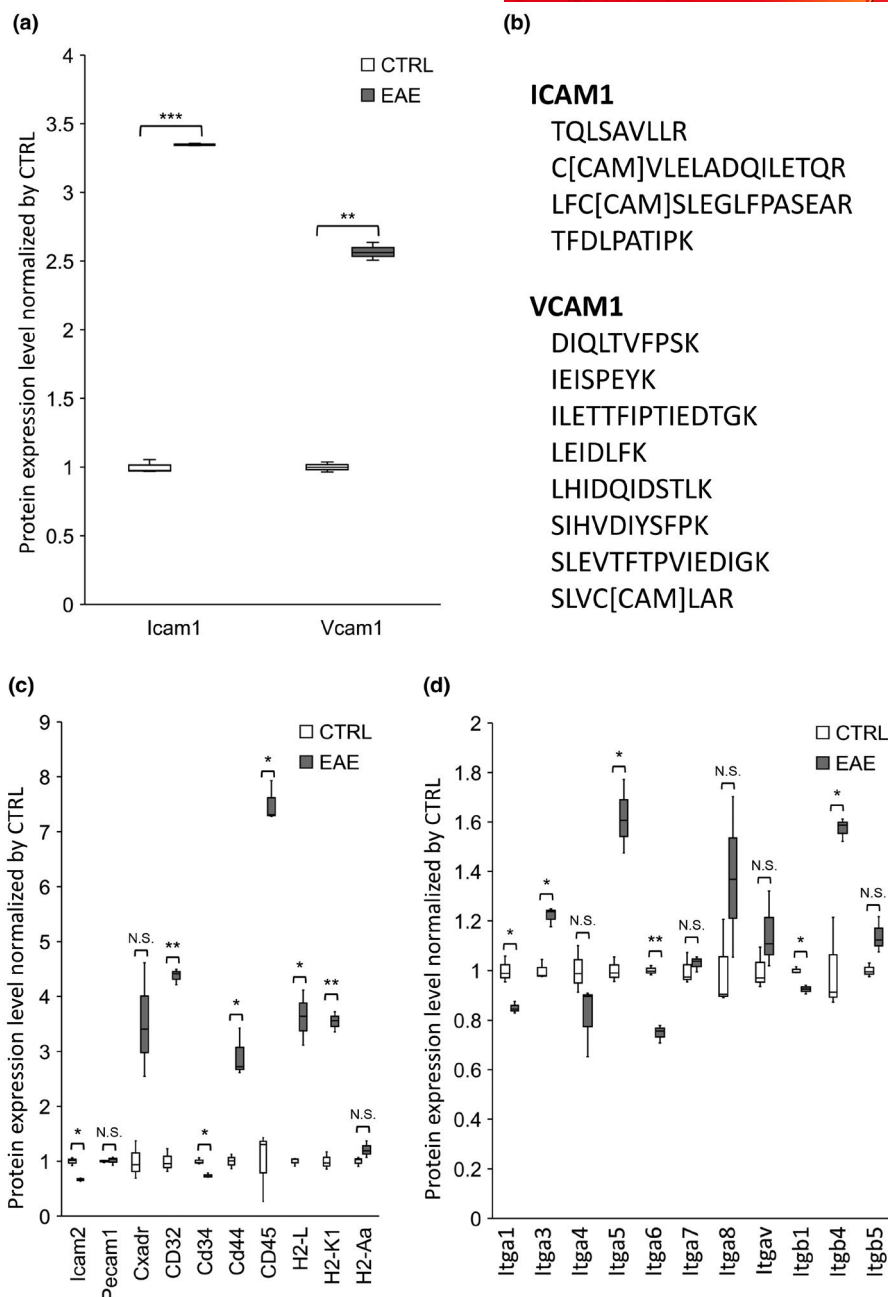


FIGURE 2 EAE-induced changes in protein expression levels of molecules related to cell infiltration in the brain capillaries. (a) Protein expression levels of ICAM1 and VCAM1 in EAE mice compared with control mice. (b) The peptide sequences used to determine the protein expression levels of ICAM1 and VCAM1. These are consistent with in silico peptide selection criteria (Uchida et al., 2013), which means that the amino acid sequences of the peptides are specific for target proteins, and the peptides are quantitatively accurate and highly sensitive without any issue in trypsin digestion. (c) Protein expression levels of other molecules reported or potentially expected to be involved in cell infiltration. (d) Protein expression levels of the integrin family. Closed box, the brain capillaries of EAE mice. Open box, the brain capillaries of control mice. The band inside the box represents the median, and the bottom and top of the box indicate the first and third quartiles, respectively. Whiskers indicate the minimum and maximum values of the protein levels ($n = 3$ independent sample processing/SWATH runs). The data are normalized by the average of protein expression level in control mice. * $p < 0.05$, ** $p < 0.01$, and *** $p < 0.001$, significantly different between EAE and control groups. N.S., not significantly different. Comparison between two groups was performed by an unpaired two-tailed Student's *t*-test, and the *p*-values were adjusted by BH correction

the Annexin A (ANXA) family were induced in EAE mice (ANXA1, 1.91-fold; ANXA2, 1.50-fold; ANXA3, 1.20-fold; ANXA4, 1.30-fold; ANXA6, 1.22-fold; ANXA7, 1.22-fold). The s100a family, which is known to form a complex with the ANXA family, also showed an

increase (s100a11, 2.03-fold; s100a16, 1.31-fold) (Figure 4a). Among the ANXA family, ANXA5, ANXA2, and ANXA6 proteins were abundantly expressed in brain capillaries isolated from EAE mice, and the expression levels of these proteins were 71.2-, 67.2-, and 57.3-fold

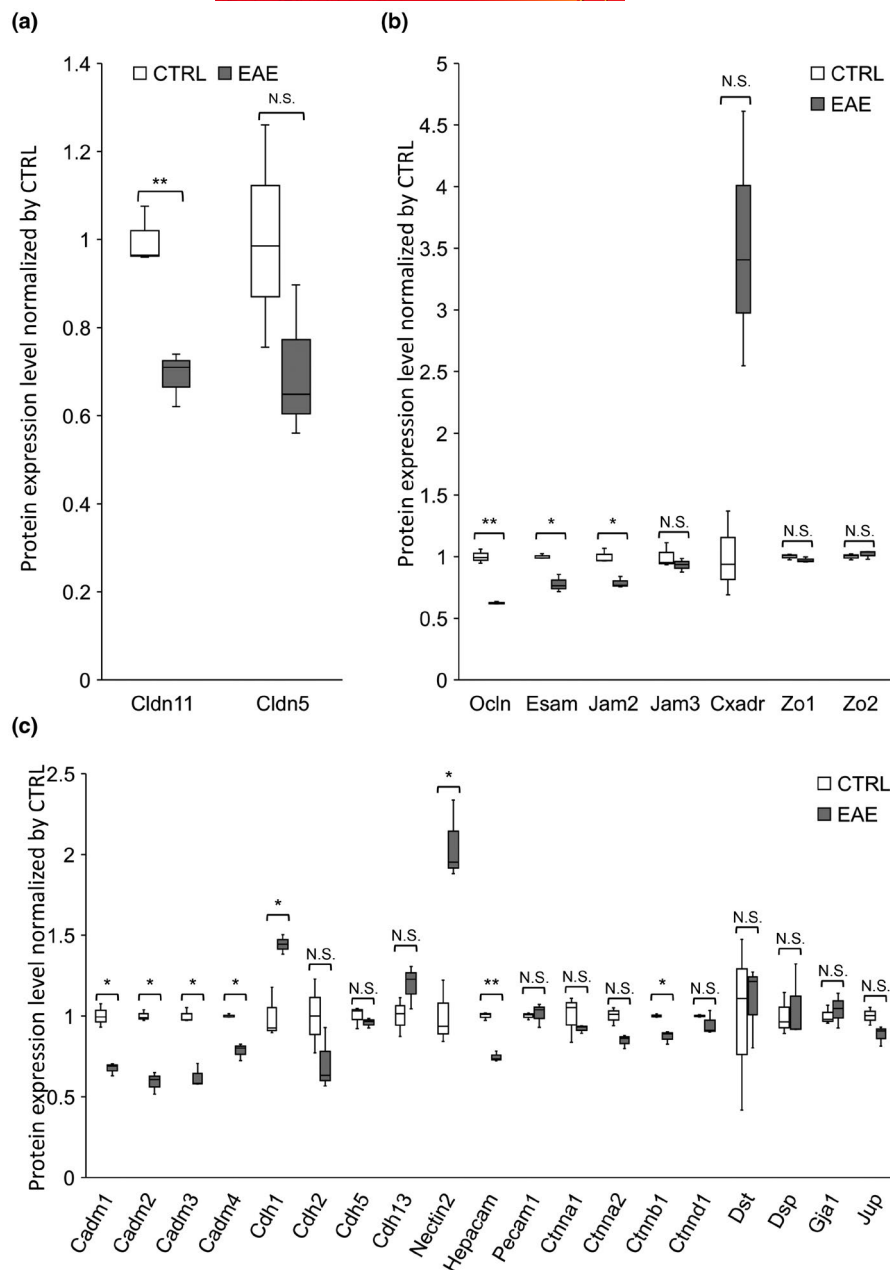


FIGURE 3 EAE-induced changes in protein expression levels of tight junction and adhesion molecules in the brain capillaries. Protein expression levels of (a) Claudin-11, Claudin-5, (b) other tight junction molecules, and (c) cell-cell junctional molecules in EAE mice compared with control mice. Closed box, the brain capillaries of EAE mice. Open box, the brain capillaries of control mice. The band inside the box represents the median, and the bottom and top of the box indicate the first and third quartiles, respectively. Whiskers indicate the minimum and maximum values of the protein levels ($n = 3$ independent sample processing/SWATH runs). The data are normalized by the average of protein expression level in control mice. * $p < 0.05$ and ** $p < 0.01$, significantly different between EAE and control groups. N.S., not significantly different. Comparison between two groups was performed by an unpaired two-tailed Student's t -test, and the p -values were adjusted by BH correction

greater than that of Claudin-5, a BBB-specific marker, respectively (Figure 4b). Among ANXA5, ANXA2, and ANXA6, the most significant up-regulation in protein expression in EAE mice was observed for ANXA2 (1.50-fold) (Figure 4a).

Because it has been reported that ANXA2 is involved in the activation of Integrin $\alpha 5$ and ICAM1, which are both involved in cell invasion and tight junction disruption, we investigated the changes in the expression of ANXA2-related molecules (Figure 5a). We detected an increase in the level of expression of the following nine proteins (Itga5, 1.62-fold; Ptp1b, 2.01-fold; Ahnak, 1.46-fold; CD44, 2.92-fold; Kindlin2, 1.53-fold; Fibronectin1, 2.74-fold; Fibrinogen alpha, 27.1-fold; Fibrinogen beta, 9.04-fold; Fibrinogen gamma, 20.4-fold) (Figure 5a). These results suggest that a series of pathways for ANXA2 are activated at the BBB during pathological conditions (Figure 5b).

3.5 | Therapeutic effect of an Annexin A2 inhibitor (LCKLSL peptide) on the pathogenesis of EAE

On the basis of the human protein atlas database (<https://www.proteinatlas.org/>), ANXA2 is selectively expressed in vascular endothelial cells in the brain (Uhlén et al., 2015). Our findings suggest that ANXA2 is a key upstream signaling molecule for cell invasion and the disruption of tight junctions. Therefore, we administered the LCKLSL peptide (5 mg/kg/day), an ANXA2 inhibitor, to EAE mice daily starting at 7 days prior to immunization. As a result, in the absence of the LCKLSL, the mice presented EAE symptom with a clinical score of 3 from Day 12 (Figure 6). In contrast, mice that had been treated with the LCKLSL peptide showed a delayed onset of EAE, with a significantly lower clinical score than the corresponding scores for the control group every

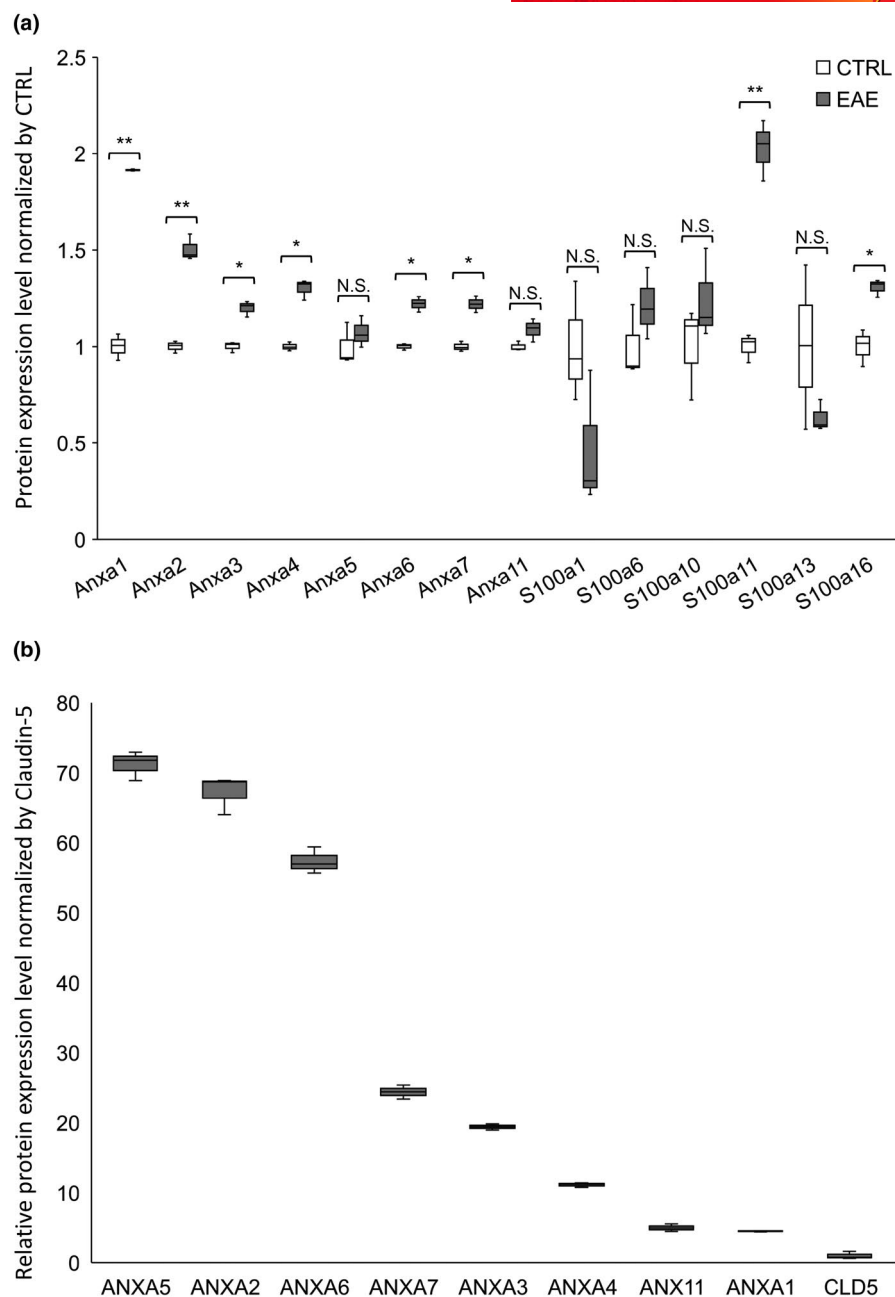


FIGURE 4 Significant up-regulation of protein expression for various members of Annexin A family and S100 family in brain capillaries isolated from EAE mice. (a) Closed box, brain capillaries of EAE mice. Open box, brain capillaries of control mice. The band inside the box represents the median, and the bottom and top of the box indicate the first and third quartiles, respectively. Whiskers indicate the minimum and maximum values of the protein levels ($n = 3$ independent sample processing/SWATH runs). The data are normalized by the average of protein expression level in control mice. * $p < 0.05$ and ** $p < 0.01$, significantly different between EAE and control groups. N.S., not significantly different. Comparison between two groups was performed by an unpaired two-tailed Student's t -test, and the p -values were adjusted by BH correction. (b) The peak area of individual Annexin members in protein level was normalized by that of BBB-specific marker protein Claudin-5 in EAE group to show the relative protein expression level. The average value of Annexin A2 was 67.2

day from Day 12 to the last day (Day 23), and EAE symptoms with a clinical score of a maximum of approximately 1 (Figure 6). Significant differences between LCKLSL peptide and vehicle groups (threshold p -value, 0.05) were determined by using two-tailed Mann-Whitney's U test (Figure 6). The details of sample metadata are described in Table S2.

4 | DISCUSSION

In the present study, for the first time, we applied the SWATH method, a highly accurate and comprehensive quantitative proteomics method to elucidate the levels of expression of pathological proteins at the BBB in a model of multiple sclerosis. It is

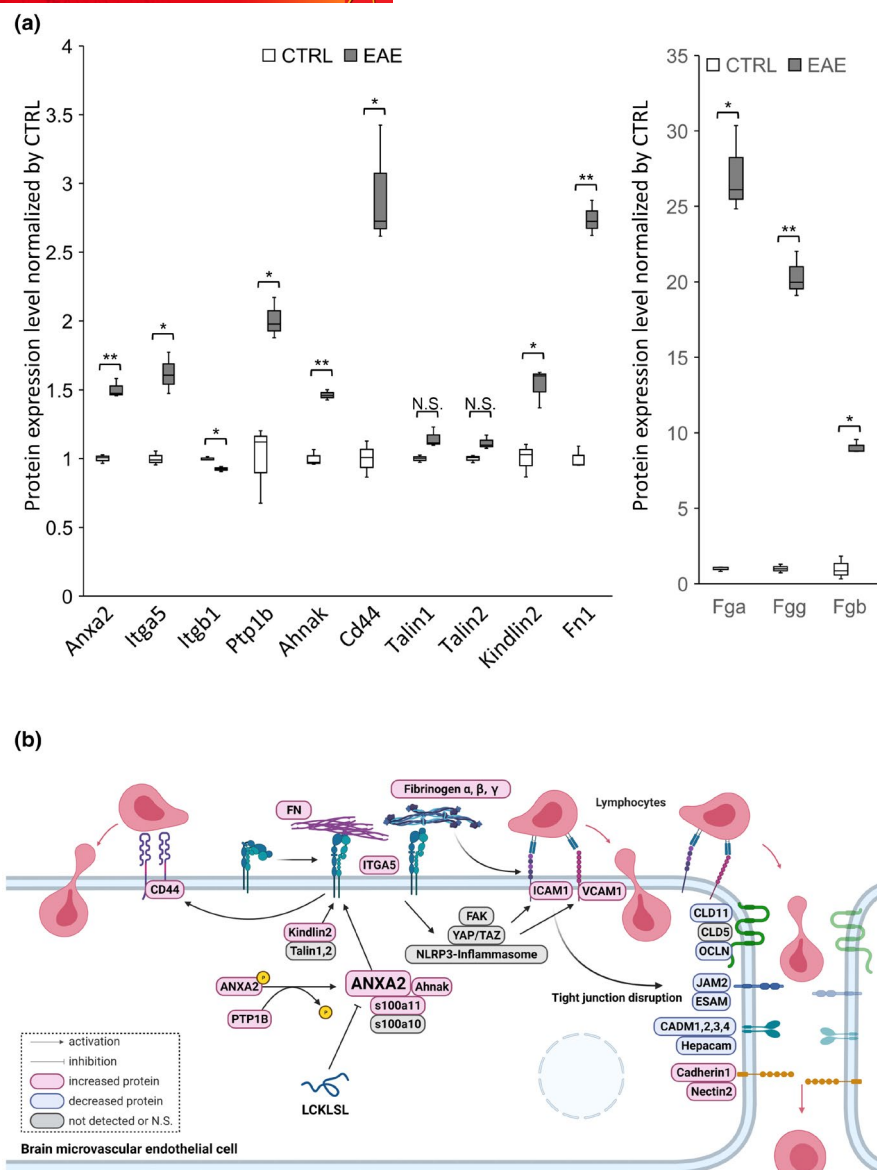


FIGURE 5 EAE-induced changes in protein expression levels of Annexin A2-related molecules and schematic illustration of molecular mechanisms leading to BBB disruption and cell infiltration in brain vascular endothelial cells. (a) Protein expression levels of Annexin A2-related molecules in EAE mice compared with control mice. Closed box, the brain capillaries of EAE mice. Open box, the brain capillaries of control mice. The band inside the box represents the median, and the bottom and top of the box indicate the first and third quartiles, respectively. Whiskers indicate the minimum and maximum values of the protein levels ($n = 3$ independent sample processing/SWATH runs). The data are normalized by the average of protein expression level in control mice. * $p < 0.05$ and ** $p < 0.01$, significantly different between EAE and control groups. N.S., not significantly different. Comparison between two groups was performed by an unpaired two-tailed Student's *t*-test, and the *p*-values were adjusted by BH correction. (b) Emerged molecular mechanisms responsible for BBB disruption and cell infiltration into brain in brain vascular endothelial cells. Annexin A2 is an upstream key player

generally thought that CD54/ICAM1 and CD106/VCAM1 at the BBB contribute to the infiltration of autoreactive lymphocytes into CNS tissue, because it was shown that the expression levels for these molecules are induced in MS patients and in EAE mice, as evidenced by immunohistochemical analyses (Bö et al., 1996; Huang et al., 2017; Steffen et al., 1994; Washington et al., 1994). In contrast, a qTAP analysis, which has a superior quantitative accuracy compared with an antibody-based analysis, has shown that the expression levels in EAE mice are nearly the same as

those in normal mice (Sato et al., 2019). However, even the qTAP method lacks accuracy because it uses a single specific peptide to quantify the target protein. In the present study, ICAM1 and VCAM1 were quantified with four and eight peptides, respectively, by a SWATH assay (Figure 2b). The results showed that ICAM1 and VCAM1 were increased by 3.3- and 2.6-fold, respectively, at the BBB of EAE mice compared with the corresponding values for control mice (Figure 2a). As shown in ICAM1 and VCAM1, we quantified the changes in the expression of target

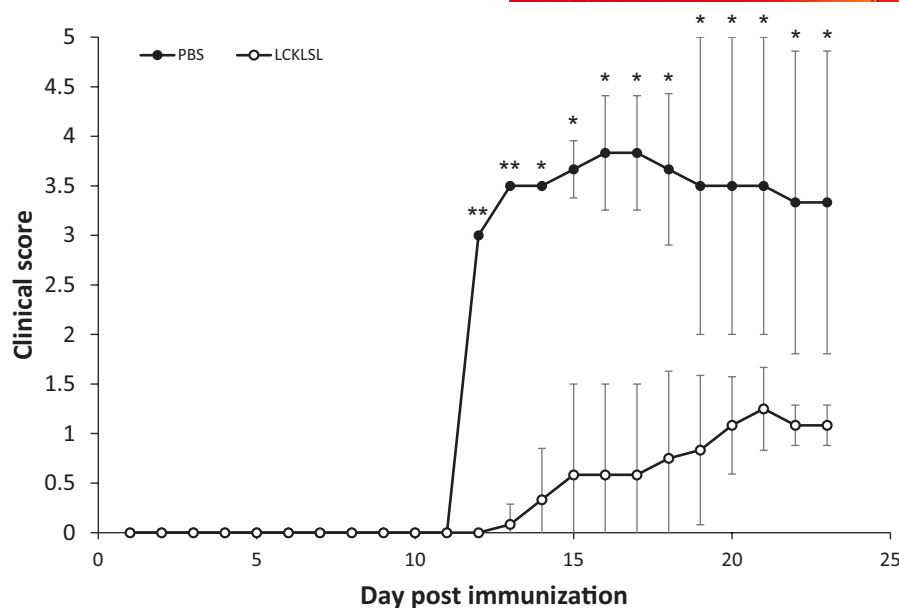


FIGURE 6 Therapeutic effect of Annexin A2 inhibitor (LCKLSL peptide) on EAE pathogenesis. Time courses for the EAE clinical scores after MOG₃₅₋₅₅ peptide immunization are shown. Twelve-week-old female C57BL/6J mice were used. Mice received intraperitoneal injections of LCKLSL peptide everyday with 5 mg/kg/day (six mice, open circle), or vehicle (PBS) for control group (three mice, closed circle), from 7 days before immunization of MOG₃₅₋₅₅ peptide. The daily injections of the LCKLSL peptide or PBS (control) were continued until Day 23 after immunization with MOG₃₅₋₅₅ peptide. EAE progression was evaluated everyday by scoring the clinical symptoms. The data are presented as the mean \pm SD. * p < 0.05, significantly different between LCKLSL peptide and vehicle groups (two-tailed Mann–Whitney's U test)

proteins by using sequences of peptides from multiple locations in the protein.

One of the more interesting findings in this SWATH study is that a series of molecules associated with Annexin A2 (ANXA2) signaling were found to be up-regulated at the BBB in EAE, representing a pathway for BBB activation (Figure 5b). The activation of Integrin $\alpha 5$ by ANXA2, which leads to the increased expression of VCAM1 and ICAM1 via FAK, has been reported to be a possible mechanism (Pang et al., 2018; Zhang et al., 2020). In the present study, protein-tyrosine phosphatase 1B (PTP1B, 2.0-fold), which activates ANXA2 via dephosphorylation (Zhang et al., 2020), and Ahnak (1.46-fold), which forms a complex with ANXA2/S100A11 and acts on actin, were both significantly up-regulated (Figure 5a). The protein expression of S100A11 (2.03-fold), which forms a complex with ANXA2 (Rintala-Dempsey et al., 2006), was also markedly increased (Figure 4a).

Increased levels of expression were also found for molecules surrounding Integrin $\alpha 5$ that are activated by ANXA2 (CD44, Talin 1, 2, and Kindlin2) (Figures 2c and 5a). It has been reported that CD44 knockout mice have a delayed onset of EAE and that lymphocyte adhesion to vascular endothelial cells is reduced (Winkler et al., 2012), suggesting that the increased expression of CD44 at the BBB shown in this study plays an important role in the pathological progression of EAE. CD44 increases the expression of Integrin $\alpha 5/\beta 1$ in basal-like breast cancer (McFarlane et al., 2015). Although a significant increase in expression levels was not observed, a slight induction for Talin 1 and 2 was found (Figure 5a). Knockdown experiments

indicate that Talin contributes to the formation of a complex between CD44 and Integrin $\beta 1$ (McFarlane et al., 2015). Kindlin2 knockout has been reported to decrease the activity of Integrin $\alpha 5/\beta 1$ (Montanez et al., 2008). These findings suggest that the expression and activity of Integrin $\alpha 5/\beta 1$ are up-regulated at the BBB of EAE and that this can be attributed to the up-regulation of Kindlin2 and CD44 (+ Talin 1 and 2).

Fibronectin (2.74-fold) and Fibrinogen (alpha, 27.1-fold; beta, 9.04-fold; gamma 20.4-fold), ligands for Integrin $\alpha 5/\beta 1$, were significantly elevated at the BBB of EAE (Figure 5a). It has been reported that fibrinogen mediates the adhesion of leukocytes to the vascular endothelium via an ICAM1-dependent pathway (Languino et al., 1993). Thus, the stimulation of Integrin $\alpha 5/\beta 1$ by Fibronectin and Fibrinogen may activate ICAM1, which is downstream from Integrin $\alpha 5/\beta 1$ and then promotes the barrier permeabilization of autoreactive lymphocytes.

On the other hand, it has also been reported that as Fibrinogen increases in brain microvascular endothelial cells (BMECs), the expression of tight junction molecules decreases and the integrity of tight junctions is lost (Patibandla et al., 2009). Although a variety of molecules have been reported to affect tight junction disruption in multiple sclerosis, the excess of fibrinogen reported in this study, alpha, 27.1-fold; beta, 9.04-fold; gamma, 20.4-fold (Figure 5a), may be major contributors to its disruption. This fibrinogen-induced decrease in the expression of tight junction molecules is inhibited by anti-ICAM1 antibodies (Patibandla et al., 2009), suggesting that the fibrinogen-induced disruption of tight junctions is mediated via the activation of ICAM1.



As a BBB tight junction molecule, in a previous study, using quantitative proteomics, we reported that Claudin-11 is highly expressed and that its expression is decreased in the BBB of EAE mice, as evidenced by immunostaining studies (Uchida et al., 2019). Because Claudin-5 is known to be the most important tight junction molecule at the BBB and has been reported to be down-regulated at the BBB of EAE mice (Argaw et al., 2009) or unchanged (Sato et al., 2019), the issue of which Claudin-11 or Claudin-5 affects BBB disruption in multiple sclerosis continues to be unclear. High-precision SWATH analysis showed that there was no significant difference in the expression of Claudin-5 between EAE and control mouse BBBs, while the expression of Claudin-11 (0.69-fold) was significantly decreased at the BBBs of EAE mice (Figure 3a). This, therefore, suggests that the decreased expression of Claudin-11, rather than Claudin-5, is more closely involved in BBB disruption in EAE. In a study of EAE induction by Argaw et al., the amounts of MOG₃₅₋₅₅ peptide (300 µg) and pertussis toxin (500 ng) administered were higher than in our experiments (MOG₃₅₋₅₅ peptide, 100 µg; pertussis toxin, 400 ng). This would induce a more pronounced form of EAE and BBB disruption. Based on these facts, we conclude that the expression of Claudin-5 was markedly reduced in the EAE mice that were used in the study by Argaw et al.

In addition to Claudin-11, the expression of occludin was decreased at the BBB of EAE (0.62-fold) (Figure 3b). Although immunostaining of occludin has been reported to reduce its signal in the spinal cords of EAE mice (Morgan et al., 2007), a quantitative analysis of the BBB was not performed. The findings reported herein show, for the first time, that Claudin-11 and Occludin are down-regulated to the same extent in the EAE BBB.

Not only tight junction molecules but the decreased expression of a number of adhesion molecules was also revealed for the first time in the BBB model of multiple sclerosis (ESAM, 0.78-fold; CADM1, 0.67-fold; CADM2, 0.59-fold; CADM3, 0.62-fold; CADM4, 0.78-fold; HEPACAM, 0.75-fold) (Figure 3c). All ESAM, CADM1, 2, 3, 4, and HEPACAM are members of the IgSFCAM family. High levels of mRNA of ESAM molecules have been reported in primary cultures of rat brain endothelial cells (Veszelska et al., 2018), and its knock-out increases vascular permeability in the lung (Duong et al., 2020). Because adhesion molecules belonging to the IgSFCAM family, such as ESAM, mediate cell–cell adhesion, the reduced expression of ESAM, CADM1, 2, 3, 4, and HEPACAM could result in an impaired cell–cell adhesion at the BBB of EAE.

In contrast, it appears that the expression of CXADR (3.5-fold), which along with ESAM, CADM, and HEPACAM, are members of the IgSFCAM family, was increased for the first time (Figure 3b). During inflammation, CXADR is up-regulated in migratory cells and has been shown to be significantly up-regulated in macrophages at the mRNA and protein levels (Nilchian et al., 2020). In the present study, the isolated vascular fraction did not contain blood cells because the vessels were perfused with PBS immediately before the isolation of the brain capillaries. This indicates that the up-regulation of CXADR at 3.5-fold (Figure 3b) likely occurs in brain capillary endothelial cells. CXADR is a protein that shows homophilically binding

(Honda et al., 2000). Therefore, it is considered that, in EAE, CXADR is up-regulated in both migrating cells and brain capillary endothelial cells, which may facilitate the adhesion of migrating cells to BMECs.

In summary, a new hypothetical molecular mechanism is proposed in which ANXA2 is positioned as a key upstream player at the BBB, and the activation of peripheral molecules such as Integrin and ICAM1 downstream of ANXA2 results in the attenuation of tight junctions and adhesion, and the infiltration of autoreactive lymphocytes and other blood cells into the CNS is promoted by the up-regulation of membrane proteins such as ICAM1, VCAM1, and CXADR (Figure 5b). Interestingly, ANXA2 is selectively expressed in vascular endothelial cells in the brain (Uhlén et al., 2015). It therefore appears that ANXA2 has the potential to serve as a therapeutic target molecule in treating multiple sclerosis by normalizing the pathological molecular mechanisms of the BBB. The LCKLSL is a peptide sequence that is contained within the ANXA2 protein and is selective for ANXA2 (Rintala-Dempsey et al., 2006). S100A11, which was up-regulated like ANXA2 (Figure 4a), forms a complex with ANXA2 and then plays an important role in the activation of ANXA2. LCKLSL is a peptide sequence at the binding domain (Rintala-Dempsey et al., 2006). In other words, it is thought that the LCKLSL peptide competitively inhibits complex formation between ANXA2 and S100A11 and thus inhibits the function of ANXA2. This leads to the hypothesis that the administration of the LCKLSL peptide to EAE mice would demonstrate the importance of ANXA2 in the pathogenesis of EAE and demonstrate the usefulness of a therapeutic strategy for targeting the BBB. Indeed, the LCKLSL peptide significantly suppressed the development of EAE, which thereby confirms our hypothesis (Figure 6). Because we cannot exclude the possibility that LCKLSL acts outside the brain to alleviate EAE, further detailed analysis will be necessary.

In conclusion, the present study was the first to comprehensively elucidate the expression of pathological proteins at the BBB in the EAE mouse model of multiple sclerosis. We found that the levels of expression of ICAM1 and VCAM1 were indeed up-regulated at the protein level and that the expression levels of Claudin-11 (not Claudin-5) and other tight junction/adhesion molecules were down-regulated. Regarding the upstream of these molecules, it was shown, for the first time, that the expression levels of ANXA2-related molecules are increased. The administration of an inhibitory peptide of ANXA2 demonstrated the importance of ANXA2 in the pathogenesis of EAE. ANXA2 is selectively and abundantly expressed in endothelial cells in the brain. It is expected that, “CNS barrier drug discovery,” which targets the molecular mechanism of the BBB, will become a useful field as a strategy for discovering new drugs for the treatment of CNS diseases.

ACKNOWLEDGMENTS

This study was supported, in part, by Grants-in-Aids from the Japan Society for the Promotion of Science (JSPS) for Scientific Research (B) [KAKENHI: 20H03399] and Fostering Joint International Research (A) [KAKENHI: 18KK0446]. This study was also supported



in part by Grants-in-Aids from the Ministry of Education, Culture, Sports, Science and Technology (MEXT) for Scientific Research on Innovative Areas [KAKENHI: 20H05495 and KAKENHI: 20H04690].

CONFLICT OF INTEREST

Yasuo Uchida is a handling editor for the *Journal of Neurochemistry*. Tetsuya Terasaki is a former handling editor of the *Journal of Neurochemistry*. The other authors declare no competing interests.

AUTHOR CONTRIBUTIONS

Kenta Tezuka conducted experiments, method development of sample preparation, analysis/acquisition of data, study design/conception, drafting of manuscript, and revision of manuscript. Masayoshi Suzuki contributed to method development of sample preparation. Risa Sato and Shohei Kawarada contributed to method development of data analysis. Tetsuya Terasaki contributed to study design/conception. Yasuo Uchida contributed to drafting of the manuscript, revision of manuscript, study design/conception, and analysis/acquisition of data.

OPEN RESEARCH BADGES



This article has received a badge for *Open Materials* because it provided all relevant information to reproduce the study in the manuscript. More information about the Open Science badges can be found at <https://cos.io/our-services/open-science-badges/>.

DATA AVAILABILITY STATEMENT

The data are available from the corresponding author upon reasonable request.

ORCID

Tetsuya Terasaki  <https://orcid.org/0000-0002-6332-7575>

Yasuo Uchida  <https://orcid.org/0000-0001-9860-1799>

REFERENCES

- Argaw, A. T., Gurfein, B. T., Zhang, Y., Zameer, A., & John, G. R. (2009). VEGF-mediated disruption of endothelial CLN-5 promotes blood-brain barrier breakdown. *Proceedings of the National Academy of Sciences of the United States of America*, 106, 1977–1982.
- Bö, L., Peterson, J. W., Mørk, S., Hoffman, P. A., Gallatin, W. M., Ransohoff, R. M., & Trapp, B. D. (1996). Distribution of immunoglobulin superfamily members ICAM-1, -2, -3, and the beta 2 integrin LFA-1 in multiple sclerosis lesions. *Journal of Neuropathology and Experimental Neurology*, 55, 1060–1072.
- Duong, C. N., Nottebaum, A. F., Butz, S., Volkery, S., Zeuschner, D., Stehling, M., & Vestweber, D. (2020). Interference with ESAM (endothelial cell-selective adhesion molecule) plus vascular endothelial-cadherin causes immediate lethality and lung-specific blood coagulation. *Arteriosclerosis, Thrombosis, and Vascular Biology*, 40, 378–393.
- Engelhardt, B., & Ransohoff, R. M. (2012). Capture, crawl, cross: The T cell code to breach the blood-brain barriers. *Trends in Immunology*, 33, 579–589.
- Gillet, L. C., Navarro, P., Tate, S., Röst, H., Selevsek, N., Reiter, L., Bonner, R., & Aebersold, R. (2012). Targeted data extraction of the MS/MS

spectra generated by data-independent acquisition: A new concept for consistent and accurate proteome analysis. *Molecular & Cellular Proteomics*, 11, O111.016717.

- Honda, T., Saitoh, H., Masuko, M., Katagiri-Abe, T., Tominaga, K., Kozakai, I., Kobayashi, K., Kumanishi, T., Watanabe, Y. G., Odani, S., & Kuwano, R. (2000). The coxsackievirus-adenovirus receptor protein as a cell adhesion molecule in the developing mouse brain. *Brain Research. Molecular Brain Research*, 77, 19–28.
- Huang, J., Han, S., Sun, Q., Zhao, Y., Liu, J., Yuan, X., Mao, W., Peng, B., Liu, W., Yin, J., & He, X. (2017). Kv1.3 channel blocker (ImKTx88) maintains blood-brain barrier in experimental autoimmune encephalomyelitis. *Cell & Bioscience*, 7, 31.
- Kamiie, J., Ohtsuki, S., Iwase, R., Ohmine, K., Katsukura, Y., Yanai, K., Sekine, Y., Uchida, Y., Ito, S., & Terasaki, T. (2008). Quantitative atlas of membrane transporter proteins: Development and application of a highly sensitive simultaneous LC/MS/MS method combined with novel in-silico peptide selection criteria. *Pharmaceutical Research*, 25, 1469–1483.
- Languino, L. R., Plescia, J., Duperray, A., Brian, A. A., Plow, E. F., Geltosky, J. E., & Altieri, D. C. (1993). Fibrinogen mediates leukocyte adhesion to vascular endothelium through an ICAM-1-dependent pathway. *Cell*, 73, 1423–1434.
- McFarlane, S., McFarlane, C., Montgomery, N., Hill, A., & Waugh, D. J. J. (2015). CD44-mediated activation of $\alpha 5\beta 1$ -integrin, cortactin and paxillin signaling underpins adhesion of basal-like breast cancer cells to endothelium and fibronectin-enriched matrices. *Oncotarget*, 6, 36762–36773.
- Montanez, E., Ussar, S., Schifferer, M., Bösl, M., Zent, R., Moser, M., & Fässler, R. (2008). Kindlin-2 controls bidirectional signaling of integrins. *Genes & Development*, 22, 1325–1330.
- Morgan, L., Shah, B., Rivers, L. E., Barden, L., Groom, A. J., Chung, R., Higazi, D., Desmond, H., Smith, T., & Staddon, J. M. (2007). Inflammation and dephosphorylation of the tight junction protein occludin in an experimental model of multiple sclerosis. *Neuroscience*, 147, 664–673.
- Nilchian, A., Plant, E., Parniewska, M. M., Santiago, A., Rossignoli, A., Skogsberg, J., Hedin, U., Matic, L., & Fuxe, J. (2020). Induction of the coxsackievirus and adenovirus receptor in macrophages during the formation of atherosclerotic plaques. *The Journal of Infectious Diseases*, 222, 2041–2051.
- Pang, D., Wang, L., Dong, J., Lai, X., Huang, Q., Milner, R., & Li, L. (2018). Integrin $\alpha 5\beta 1$ -Ang1/Tie2 receptor cross-talk regulates brain endothelial cell responses following cerebral ischemia. *Experimental & Molecular Medicine*, 50, 1–12.
- Patibandla, P. K., Tyagi, N., Dean, W. L., Tyagi, S. C., Roberts, A. M., & Lominadze, D. (2009). Fibrinogen induces alterations of endothelial cell tight junction proteins. *Journal of Cellular Physiology*, 221, 195–203.
- Rintala-Dempsey, A. C., Santamaria-Kisiel, L., Liao, Y., Lajoie, G., & Shaw, G. S. (2006). Insights into S100 target specificity examined by a new interaction between S100A11 and annexin A2. *Biochemistry*, 45, 14695–14705.
- Rossi, B., Angiari, S., Zenaro, E., Budui, S. L., & Constantin, G. (2011). Vascular inflammation in central nervous system diseases: Adhesion receptors controlling leukocyte-endothelial interactions. *Journal of Leukocyte Biology*, 89, 539–556.
- Sato, K., Tachikawa, M., Watanabe, M., Uchida, Y., & Terasaki, T. (2019). Selective protein expression changes of leukocyte-migration-associated cluster of differentiation antigens at the blood-brain barrier in a lipopolysaccharide-induced systemic inflammation mouse model without alteration of transporters, receptors or tight junction-related protein. *Biological & Pharmaceutical Bulletin*, 42, 944–953.
- Steffen, B. J., Butcher, E. C., & Engelhardt, B. (1994). Evidence for involvement of ICAM-1 and VCAM-1 in lymphocyte interaction with endothelium in experimental autoimmune encephalomyelitis in the



- central nervous system in the SJL/J mouse. *The American Journal of Pathology*, 145, 189–201.
- Uchida, Y., Goto, R., Takeuchi, H., Łuczak, M., Usui, T., Tachikawa, M., & Terasaki, T. (2020a). Abundant expression of OCT2, MATE1, OAT1, OAT3, PEPT2, BCRP, MDR1, and xCT transporters in blood-arachnoid barrier of pig and polarized localizations at CSF- and blood-facing plasma membranes. *Drug Metabolism and Disposition*, 48, 135–145.
- Uchida, Y., Higuchi, T., Shirota, M., Kagami, S., Saigusa, D., Koshiba, S., Yasuda, J., Tamiya, G., Kuriyama, S., Kinoshita, K., Yaegashi, N., Yamamoto, M., Terasaki, T., & Sugawara, J. (2021). Identification and validation of combination plasma biomarker of afamin, fibronectin and sex hormone-binding globulin to predict pre-eclampsia. *Biological & Pharmaceutical Bulletin*, 44, 804–815.
- Uchida, Y., Sasaki, H., & Terasaki, T. (2020b). Establishment and validation of highly accurate formalin-fixed paraffin-embedded quantitative proteomics by heat-compatible pressure cycling technology using phase-transfer surfactant and SWATH-MS. *Scientific Reports*, 10, 11271.
- Uchida, Y., Sumiya, T., Tachikawa, M., Yamakawa, T., Murata, S., Yagi, Y., Sato, K., Stephan, A., Ito, K., Ohtsuki, S., Couraud, P. O., Suzuki, T., & Terasaki, T. (2019). Involvement of claudin-11 in disruption of blood-brain, -spinal cord, and -arachnoid barriers in multiple sclerosis. *Molecular Neurobiology*, 56, 2039–2056.
- Uchida, Y., Tachikawa, M., Obuchi, W., Hoshi, Y., Tomioka, Y., Ohtsuki, S., & Terasaki, T. (2013). A study protocol for quantitative targeted absolute proteomics (QTAP) by LC-MS/MS: Application for inter-strain differences in protein expression levels of transporters, receptors, claudin-5, and marker proteins at the blood-brain barrier in ddY, FVB, and C57BL/6J mice. *Fluids Barriers CNS*, 10, 21.
- Uchida, Y., Yagi, Y., Takao, M., Tano, M., Umetsu, M., Hirano, S., Usui, T., Tachikawa, M., & Terasaki, T. (2020c). Comparison of absolute protein abundances of transporters and receptors among blood-brain barriers at different cerebral regions and the blood-spinal cord barrier in humans and rats. *Molecular Pharmaceutics*, 17, 2006–2020.
- Uhlén, M., Fagerberg, L., Hallström, B. M., Lindskog, C., Oksvold, P., Mardinoglu, A., Sivertsson, Å., Kampf, C., Sjöstedt, E., Asplund, A., Olsson, I. M., Edlund, K., Lundberg, E., Navani, S., Szigartyo, C. A., K., Odeberg, J., Djureinovic, D., Takanen, J. O., Hober, S., ... Pontén, F. (2015). Proteomics. Tissue-based map of the human proteome. *Science*, 347, 1260419.
- Veszelka, S., Tóth, A., Walter, F. R., Tóth, A. E., Gróf, I., Mészáros, M., Bocsik, A., Hellinger, É., Vastag, M., Rákhely, G., & Deli, M. A. (2018). Comparison of a rat primary cell-based blood-brain barrier model with epithelial and brain endothelial cell lines: Gene expression and drug transport. *Frontiers in Molecular Neuroscience*, 11, 166.
- Washington, R., Burton, J., Todd, R. F., III, Newman, W., Dragovic, L., & Dore-Duffy, P. (1994). Expression of immunologically relevant endothelial cell activation antigens on isolated central nervous system microvessels from patients with multiple sclerosis. *Annals of Neurology*, 35, 89–97.
- Winkler, C. W., Foster, S. C., Matsumoto, S. G., Preston, M. A., Xing, R., Bebo, B. F., Banine, F., Berny-Lang, M. A., Itakura, A., McCarty, O. J. T., & Sherman, L. S. (2012). Hyaluronan anchored to activated CD44 on central nervous system vascular endothelial cells promotes lymphocyte extravasation in experimental autoimmune encephalomyelitis*. *The Journal of Biological Chemistry*, 287, 33237–33251.
- Zhang, C., Zhou, T., Chen, Z., Yan, M., Li, B., Lv, H., Wang, C., Xiang, S., Shi, L., Zhu, Y., & Ai, D. (2020). Coupling of integrin $\alpha 5$ to annexin A2 by flow drives endothelial activation. *Circulation Research*, 127, 1074–1090.

SUPPORTING INFORMATION

Additional supporting information may be found in the online version of the article at the publisher's website.

How to cite this article: Tezuka, KP, Suzuki, M, Sato, R, Kawarada, S, Terasaki, T, Uchida, Y (2022) Activation of Annexin A2 signaling at the blood–brain barrier in a mouse model of multiple sclerosis. *Journal of Neurochemistry*. 160:662–674. <https://doi.org/10.1111/jnc.15578>